

OBSERVATIONS OF NEUTRAL HYDROGEN IN THE GALACTIC PLANE IN THE LONGITUDE INTERVAL -6° TO 120°

W. B. BURTON
Leiden Observatory

Received March 23, 1970

The 25-m Dwingeloo telescope has been used to obtain 21-cm line profiles in the galactic plane in the range of longitude -6° to 120° . The line profiles are reproduced graphically as Part V of the "Dwingeloo Atlas of 21-cm Profiles". The observations are also presented on two contour maps of brightness temperatures in velocity-longitude coordinates. The terminal positive velocity and the integrated brightness of the profiles are tabulated. The astronomical discussion of the observations is given elsewhere. The standard reduction procedures applied to Dwingeloo hydrogen-line measurements made since June 1967 are summarized.

1. REDUCTION OF DWINGELOO LINE PROFILES

1.1. Introduction

All 21-cm line profiles observed with the 25-m radio telescope in Dwingeloo since June 1967 have been reduced with newly designed programs on the IBM 360/50 computer of the University of Leiden. The reduction procedures for measurements made before the change to this computer have been described by Raimond (1966) and by Muller *et al.* (1966). The redesigned standard reduction programs allow almost completely automatic reduction of the measurements. They are described in detail in a handbook written in Dutch by Hoekema (1969). This handbook contains a summary written in English and is available from Leiden Observatory.

The telescope and the parametric amplifier have been described elsewhere (Westerhout 1958 and Muller *et al.* 1966). Since July 1964 the parametric amplifier has been used with a 20-channel receiver (see de Boer *et al.* 1968) designed by C. A. Muller and the staff of the Dwingeloo Radio Observatory.

The width at 1420 MHz of the main lobe of the antenna pattern between half-power points is $0^{\circ}.58$ in the horizontal plane and $0^{\circ}.63$ in the vertical one. The antenna pattern has recently been determined by Hartsuijker *et al.* (1970).

The 20-channel receiver can be operated with intermediate-frequency stage bandwidths of 8, 16 or 50 kHz. The 20 channels are spaced by 50 kHz. By tuning the frequency of a local oscillator, all 20 channels scan 110 kHz of the spectrum, so that each channel overlaps more than half of the next one. The result is a profile about 1000 kHz long. The tuning-rate is $10.5 \text{ kHz min}^{-1}$ for 8 kHz bandwidth and 21 kHz min^{-1} for 16 kHz bandwidth. Either tuning-rate may be chosen for the 50 kHz broadband measurements. The channel outputs pass through filters with time constants of 10 seconds and are sampled every 6.6 seconds.

Practice has shown that about 70 slow tuning-rate and 100 fast tuning-rate measurements can be made in 24 hours, in addition to the necessary instrumental measurements.

The reduction programs are intended to be almost completely automatic. Thus they contain provisions for localizing, analysing, and, if possible, correcting a large variety of errors in the measurements. The programs report all the errors found and indicate what action, if any, has been taken. The reduction processes are summarized below.

The channel output samples are recorded digitally on punched paper tape. The content of the paper tape is checked for parity errors and internal inconsistencies and is rewritten on magnetic tape in a standardized form.

1.2. Positions and times

The positions (altitude, azimuth, right ascension, declination) and the times (siderial time, universal time, Julian day) are recorded at the beginning and at the end of each observation. A check is made on the internal consistency of the positions and times. The changes of the positions and times during the course of the observations are also checked. If internal inconsistencies or unexpected changes are found, an attempt is made to localize and repair the suspect quantity, making use of the available redundancy; an error report is made and the reduction continues. The average position and time for the measurement are calculated. A correction for the flexure of the telescope and for refraction is applied to the telescope settings. The desired coordinates (which are assumed to be $l^{\text{II}}, b^{\text{II}}$ unless $l^{\text{I}}, b^{\text{I}}$ or α, δ are specified) are calculated from the corrected right ascension and declination. The epochs used are always within one half year of the date of observation. Under normal conditions the setting accuracy of the telescope is $0^{\circ}.03$ (see Westerhout 1958 and van Woerden 1962).

1.3. Frequencies

A check is made on the recorded frequencies to establish if the individual frequencies within each channel increase linearly as expected. If errors are located they are generally corrected by linear interpolation and an error report is given. A similar check is made to verify that the channels are labelled correctly; the programs are designed to accept the output of a receiver with an arbitrary number of channels.

The frequencies are converted to velocities (km s^{-1}) with respect to the local standard of rest making use of the formulas of MacRae and Westerhout (1956). A time-constant correction is made for the delay of the signal in the low-pass filter.

1.4. Intensities

A check is made to see if the recorded intensities in any channel change unexpectedly. If an unexpected change in the intensities is found, the error is analysed and eventually corrected by linear interpolation, with suitable error reports. If an intensity is repaired by interpolation it carries reduced weight during the remaining reduction.

The recorded intensities are smoothed by averaging with a suitable weighting function over intervals of approximately 1 or 2 km s^{-1} . These intervals are approximately 1 km s^{-1} long for 8 kHz bandwidth measurements and for measurements made with 50 kHz bandwidth and the slow tuning rate. The intervals are approximately 2 km s^{-1} long for the other measurements. The 1 km s^{-1} intervals are centered at integral velocities; the 2 km s^{-1} intervals are centered at integral multiples of 2 km s^{-1} .

Special measurements are made about six times per day to determine the zero-levels (dc levels) of the low-frequency section of the receiver. These measurements are reduced separately, with appropriate checks

and corrections, to obtain an array containing the weighted values of the various channels' low-frequency zero-levels, extending over a period of several weeks. The low-frequency zero-level found for each channel by linear interpolation in time in this array is subtracted from the intensities.

Similarly, special measurements are made about eight times per day of the relative sensitivity of the various channels. The intensities are multiplied by the relative sensitivity factors found by interpolation in an array of several weeks length. After this correction the intensity scale is the same for all channels.

The intensities are corrected for atmospheric extinction. The extinction and other corrections are given explicitly by Hoekema (1969).

A correction is applied to account for the reduction of receiver sensitivity caused by continuum radiation from the ground, air and sky. This correction factor is determined by measuring the total noise simultaneously with every observation.

No correction for scattered radiation is applied in the standard reduction.

The intensities are converted from recorder divisions to Dwingeloo units where 1 unit ≈ 1 °K (see Volders and Högbom 1961).

The channels generally overlap partially in velocity. A weighted average of intensities in overlapping channels is taken. If individual intensities differ from the average intensity by more than 1.2, 1.0 or 0.7 °K for bandwidths 8, 16 or 50 kHz respectively, an error report is given. If the deviating point can be identified, it is discarded, not repaired; all these deviating points are presented in a table for detailed study by the astronomer.

The zero-level of the intensity scale, corresponding to zero emission, is calculated from observations made in the standard zero-level fields listed in table 1. The fields were chosen as ones at which only little emission is present. Measurements of zero-level fields are made about 25 times per day. The velocity range observed is chosen to provide complete coverage of the normal measurements being made during that observing period. The zero-level measurements are reduced as normal measurements.

Table 1. Standard Dwingeloo zero-level fields

Field	l	b	Field	l	b
0*	123°	+ 27.3	4	62°	+ 40°
1	90	+ 40	5	90	- 70
2	130	- 24	6	232	+ 19
3	184	+ 35	7	355	+ 30

*at $\delta = 90^\circ$.

The zero-level brightness temperature T_{bz} at a velocity V_z has been found empirically (see Muller *et al.* 1966) to be a function of Julian day JD, altitude A , and temperature T_K at the receiver front-end. The dependences on these parameters are found by the least-squares method from the zero-field measurements. A representative zero-line is

$$T_{bz}(V_z) = C_1(V_z) + C_2(V_z)(T_{K0} - T_{K0}) + C_3(V_z)(A - A_0) + C_4(V_z)(JD - JD_0). \quad (1)$$

The term $C_1(V_z)$ dominates.

The fiducial field at $l = 132^\circ$, $b = -1^\circ$ is measured several times during each of three different periods per day. These measurements are made in order to determine the small changes in the intensity scale due to variations from unknown causes in the characteristics of the equipment. A check is first made to see that the

observed coordinates do not vary by more than $0^{\circ}.1$ from those of the fiducial field. After reduction as a normal measurement, the sensitivity measurements are compared with a defined standard measurement of this field. The comparison is done by a least-squares analysis and results in two quantities for each sensitivity measurement, namely an intensity scale-factor and a velocity-shift measure. These quantities are arrayed in order of time. The correction factors to be applied to each normal measurement are determined by linear interpolation in this array.

Examination of several hundred of the sensitivity and velocity-shift corrections applied to measurements made during 1969 indicates that the intensity scale of Dwingeloo profiles is internally consistent to within about one per cent, and that the velocities are stable to within about $\pm 0.05 \text{ km s}^{-1}$. The absolute intensity scale may differ by 10 to 20 per cent from true degrees Kelvin (see van Woerden *et al.* 1962). The sensitivity and velocity-shift corrections were not applied to measurements reduced with these programs before 1969.

Finally the intensities of the 50 kHz bandwidth measurements are expressed at multiples of 5 or 10 km s^{-1} respectively for slow and fast tuning-rates, by taking a weighted average in intervals approximately 5 or 10 km s^{-1} long.

At the request of the astronomer, the reduced measurements can be sorted on magnetic tape, punched on cards, plotted in a variety of ways with a CalComp plotter, or listed together with all error reports. The computer time necessary to reduce one measurement is about 0.8 minutes. Generally six weeks pass before the end of an observing period and the completion of the entire reduction.

1.5. Statistical fluctuations

The error estimate which is of most direct interest to the observer is the expected root-mean-square deviation of a single point in a completely reduced measurement. Fluctuations in the intensities on the profiles' wings, where no emission is evident, represent error due primarily to receiver noise, although error due to other sources such as scattered radiation, poorly determined relative channel sensitivities, or possible low-level emission, may also be present. The r.m.s. deviation for 8 kHz bandwidth measurements was determined from 60 points on the extreme 60 km s^{-1} of 150 measurements selected from the observations described in section 2. The 150 measurements represent observations made throughout the 1969 observing period. Measurements made in the direction of continuum sources were not used in the noise determination. The average r.m.s. deviation for the measurements is $\mu(T_b) = 0.51^{\circ}\text{K}$. A. N. M. Hulsbosch (private communication) has determined the r.m.s. deviation for 50 kHz bandwidth measurements made during the same observing period. He used 10 points covering 50 km s^{-1} on the wings of 10 measurements and found an average r.m.s. deviation $\mu(T_b) = 0.10^{\circ}\text{K}$. A representative value of the r.m.s. deviation in a 16 kHz bandwidth measurement follows from the value found empirically for the 8 kHz measurements. The noise to be expected in Dwingeloo profiles is summarized in table 2.

Table 2. Empirically determined noise in Dwingeloo profiles

Bandwidth (kHz)	$\mu(T_b)$ ($^{\circ}\text{K}$)
8	0.51
16	0.36
50	0.10

The standard reduction programs were designed and written by W. N. Brouw, W. B. Burton, T. Hoekema,

Y. W. Kroodsmas, J. van Kuilenburg, J. Oostindier, J. J. Schafgans, W. W. Shane and H. W. van Someren-Greve. The reduction is the responsibility of J. W. Brotherhood, P. Katgert, Y. W. Kroodsmas and P. R. Wesselius. The observations are done under the supervision of the Chief Observer H. Meijer and R. Sancisi. The Radio Observatory at Dwingeloo is supported by the Netherlands Organization for the Advancement of Pure Research (Z. W. O.).

2. OBSERVATIONS IN THE GALACTIC PLANE

The region of the galactic plane in the range $-6^\circ \leq l \leq 120^\circ$ has been observed at half-degree intervals of longitude, using 8 kHz bandwidth. The observations were made in order to obtain a reference map and a complete set of terminal velocities for this part of the galactic plane. The material is used in a subsequent paper as an aid in interpretation of galactic structure based on various kinematic models.

The measurements were made during March and June 1969. Each measurement covers a velocity range of 220 km s^{-1} . At each position at least two partly overlapping measurements are necessary in order to cover all velocities at which emission is present and to include zero-levels about 80 km s^{-1} long on each side of the emission. In the directions $l \leq 12^\circ$ three partly overlapping measurements are necessary to cover the entire emission range with suitable zero-level wings. Each position was measured several times, generally including at least one measurement in each of the two observing periods. Column 2 of table 3 gives the coverage of each profile: the first digit is the number of successful measurements averaged to obtain the low-velocity side of the profile and the last digit is the same for the high-velocity side. For $l \leq 12^\circ$, the middle digit is the number of measurements averaged to obtain the central part of the profile.

A check was made on the position of each measurement. All measurements made at longitudes deviating from integral multiples of one-half degree by more than $0^\circ.05$ were discarded, as were all measurements made at $|b| > 0^\circ.05$. Before the measurements were averaged a final adjustment was made to the zero-level. The correction consisted in subtracting a constant from all intensities in a measurement, the constant being the weighted average of all intensities on the extreme 60 km s^{-1} of the wing of the measurement. The correction was not applied to the intermediate velocity measurements at $l \leq 12^\circ$ because these observations do not have long wings with no emission. The correction was not applied to profiles at $l \leq 6^\circ$, because the zero-level wings on these profiles are not uniformly flat for the first and last 60 km s^{-1} . This zero-level distortion is due to the fact that the measured profile extends over a velocity range larger than the velocity separation of 456 km s^{-1} between the receiver's signal and comparison bands. Hydrogen emission is present over such a large velocity range in directions $l \leq 6^\circ$ that emission can be detected in a comparison channel. This leads to the recorded negative intensities seen on the extreme wings of some profiles. The average value of this zero-level correction, determined from a sample of 100 measurements made throughout the observing period, was $\pm 0.22^\circ \text{K}$. The correction varied around zero, which together with its small magnitude and the generally flat appearance of the profiles' zero-level, indicates that the intensity zero-line has been adequately determined. Although the observations have not been explicitly corrected for scattered radiation, the final adjustment to the zero-level serves to remove the broad weak base of the scattered radiation profile.

In calculating the weighted average of overlapping measurements, the mean deviation of the intensities of the individual measurement from the average profile at that longitude was found. This quantity was used to detect any measurements of poor quality which had escaped detection beforehand.

The line profiles reproduced below form Part V of the "Dwingeloo Atlas of 21-cm Profiles". The ordinate of the graphs is expressed in the brightness-temperature units defined by Volders and Högbom (1961), where 1 unit $\approx 1^\circ \text{K}$. The scale is $100^\circ \text{K} = 2 \text{ cm}$. The abscissa is expressed in km s^{-1} with respect to the local standard of rest. The scale of the abscissa is such that $100 \text{ km s}^{-1} = 5 \text{ cm}$. The observations are shown as

points at intervals of 1 km s^{-1} . The profiles could be made available in tabular or in machine-readable form on request. The observations extend in fact over a somewhat larger velocity range than that indicated by the atlas; the minimum and maximum velocities observed are given in columns 2 and 3 of table 4. However, portions of profiles omitted from the atlas show no significant deviations from the zero-level. The r.m.s. error in the intensities is approximately $0.5 \text{ }^\circ\text{K}$ divided by the square root of the coverage factor in column 2 of table 3. However, observations made in the directions $l < 5^\circ$ have mean errors at least twice as large as those of the other measurements. This increase in noise is due to the necessary low altitude of observation. All observations in directions $l > 6^\circ$ were made with the telescope set at altitudes higher than 10° . In the directions closer to that of the galactic center the minimum allowed altitude was 3° , although in practice it was rarely less than 5° .

Profiles in directions $l \leq 3^\circ$ are spaced further apart in the atlas so that the absorption dips in successive profiles do not overlap. The peak in some of the profiles at very high velocity (for example at $l \leq 12^\circ$, $V \approx 250 \text{ km s}^{-1}$) is due to a leak in the parametric amplifier. This peak is easily recognized on the profiles because of its sharpness and high velocity, so that it cannot be mistakenly interpreted as hydrogen emission. That some of the profiles show multiple peaks is due to the fact that several measurements were averaged to obtain each atlas profile. Since the leak occurs at a fixed instrumental frequency, it will occur, after correction to the local standard of rest, at different velocities in measurements made at different times.

Contour maps were prepared from the line profiles. The neutral hydrogen in the galactic plane between $l = -6^\circ$ and $l = 120^\circ$ is represented in figure 1. Neutral hydrogen in the region $-6^\circ \leq l \leq 16^\circ$ is represented by a contour map in figure 2. Figures 1 and 2 are to be found in the envelope bound into the journal after page 338. The contour maps and the line profiles were drawn using a routine written by S. C. Simonson and were prepared for publication by J. P. M. Kluiters.

In figure 2 intensities of about $2 \text{ }^\circ\text{K}$ are seen extending between -225 km s^{-1} and -255 km s^{-1} in the direction $l = 0^\circ.0$. Although these intensities are present on all the relevant measurements, caution is suggested by coincidence between the direction of these intensities and the strong continuum source Sagittarius A, as well as by the weakness of the intensities in a region of increased noise due to low observing altitude, and by the absence of these intensities at the adjacent longitudes $l = \pm 0^\circ.5$. A special series of measurements is being undertaken to examine the reality of these intensities.

Several small-scale features with unique velocities are evident in figure 1. Four of these features are centered, respectively, as follows: $l = 75^\circ$ at $V = -130 \text{ km s}^{-1}$, $l = 84^\circ.5$ at $V = +45 \text{ km s}^{-1}$, $l = 75^\circ.5$ at $V = +40 \text{ km s}^{-1}$ and $l = 106^\circ.0$ at $V = -130 \text{ km s}^{-1}$. These four features are evident on several measurements made during both observing periods. Measurements at latitudes other than $b = 0^\circ$ are necessary for a detailed study of these features. Such observations have been included in the Dwingeloo observing program.

The terminal velocity was calculated for the profiles in directions $l \geq 16^\circ$, where it can be interpreted in terms of galactic rotation. The terminal velocity is defined as the velocity of the highest-velocity maximum ($T_b > 30 \text{ }^\circ\text{K}$) on the profile plus the width of an equivalent rectangle. This rectangle has the same height as the highest-velocity maximum and a width such that the area of the rectangle is the same as the area under that part of the profile with velocities greater than the velocity of the highest-velocity maximum. This is the same measure of the terminal velocity as used by Shane and Bieger-Smith (1966) in their rotation-curve work. The terminal velocities are tabulated in column 3 of table 3.

The integrated brightness was determined for each profile. The integrated brightness under the negative-velocity part and under the positive-velocity part of the observed profiles are tabulated in columns 4 and 5, respectively, of table 3.

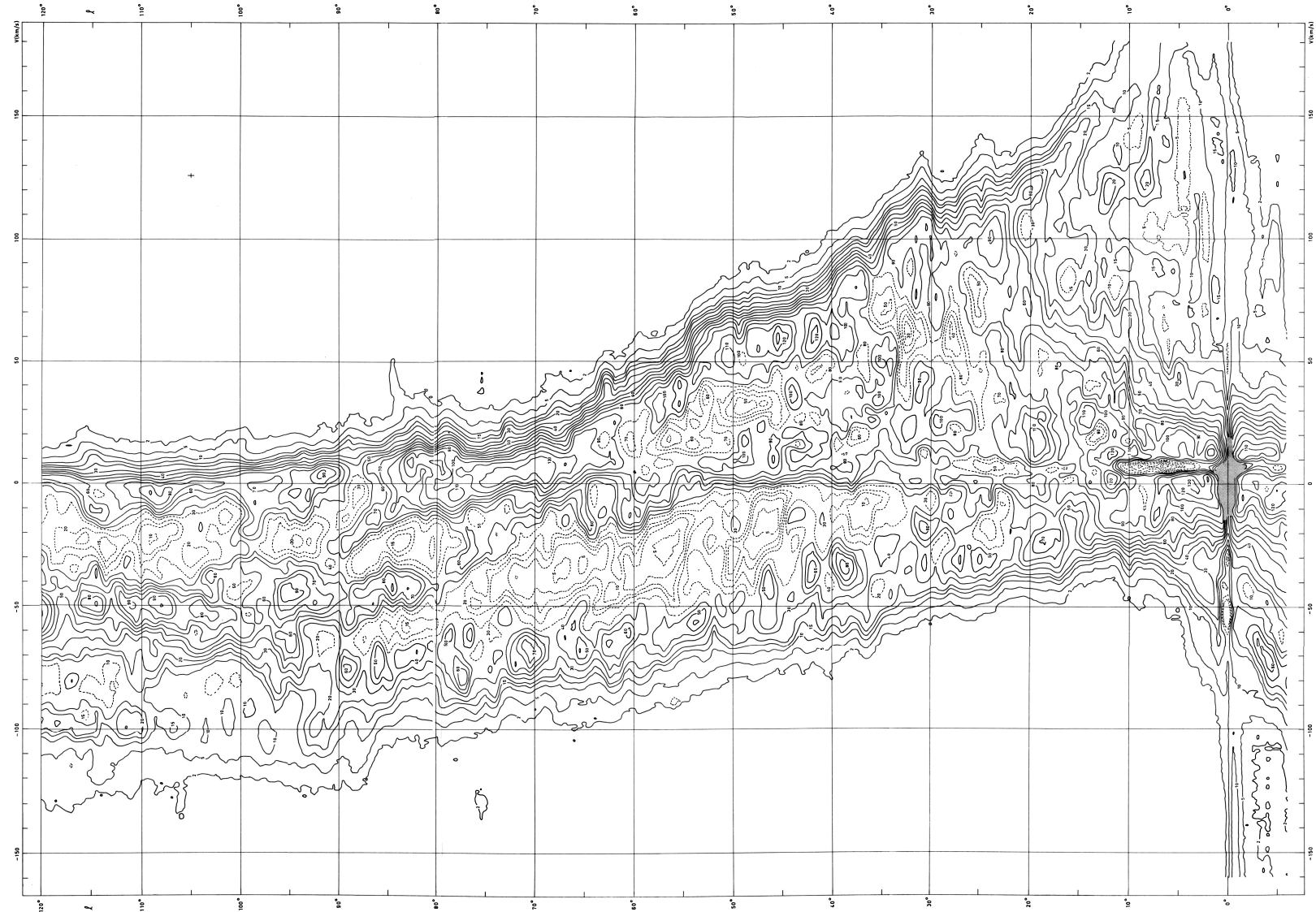


Figure 1. Neutral hydrogen in the galactic plane in the longitude interval -6° to 120° . Brightness-temperature contours are drawn at 2°K, 5°K, 10°K, 15°K, 20°K, 30°K, etc. Broken-line contours enclose regions of relatively low brightness temperatures. The velocity, v , with respect to the local standard of rest. The bandwidth (1.7 km s⁻¹) and half-power beamwidth (0.6°) are indicated by the cross in the upper left-hand corner. The shaded portion of the map is a region of low brightness temperature.

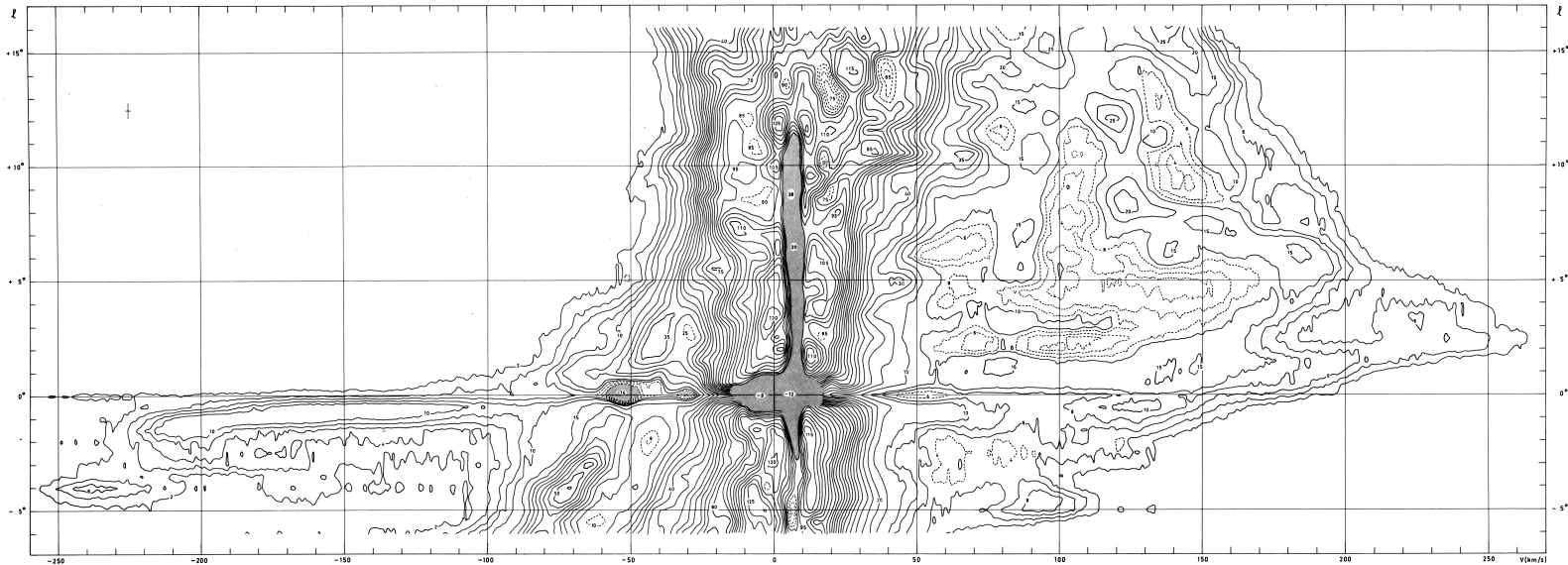
OBSERVATIONS OF NEUTRAL HYDROGEN IN THE GALACTIC PLANE IN THE LONGITUDE INTERVAL -6° TO 120° W. B. Burton 1970, *Astr. Astrophys. Suppl.*, 2, 261.

Figure 2. Neutral hydrogen in the galactic plane in the longitude interval -6° to 16° . Brightness-temperature contours are drawn at steps of 2°K for $T_b < 10^{\circ}\text{K}$ and at 5°K steps for higher temperatures. Broken-line contours enclose regions of relatively low brightness temperatures. The velocity is with respect to the local standard of rest. The bandwidth (1.7 km s^{-1}) and the half-power beamwidth ($0'.6$) are indicated by the cross in the upper left-hand corner. The shaded portions of the map are regions of absorption where contour lines would be overcrowded due to steep temperature gradients. Depths of absorption dips are indicated in the shaded regions. Observations are spaced at half-degree intervals of longitude.

Table 3. Coverages, terminal velocities, integrated brightness at negative velocities and integrated brightness at positive velocities

l	Cov.	V_t (km s^{-1})	B_n ($^{\circ}\text{K km s}^{-1}$)	B_p	l	Cov.	V_t (km s^{-1})	B_n ($^{\circ}\text{K km s}^{-1}$)	B_p	l	Cov.	V_t (km s^{-1})	B_n ($^{\circ}\text{K km s}^{-1}$)	B_p
-6.0	122		5189	2581	19.0	23	130.5	2202	8436	44.0	12	73.7	1890	6916
-5.5	222		4651	2680	19.5	33	130.2	2106	8723	44.5	21	72.3	1894	6791
-5.0	223		4795	3188	20.0	23	128.9	2044	8724	45.0	32	72.0	1635	6541
-4.5	223		5061	3316	20.5	34	127.5	2067	8442	45.5	31	71.3	1544	6594
-4.0	223		5053	3259	21.0	34	126.9	1878	8042	46.0	32	71.8	1897	6571
-3.5	213		4508	3075	21.5	34	124.1	1768	8182	46.5	31	71.7	2070	6452
-3.0	213		4378	3141	22.0	34	121.1	1764	8600	47.0	32	71.3	1822	6405
-2.5	212		3926	3249	22.5	33	120.5	1540	8703	47.5	32	71.5	1456	6544
-2.0	112		3932	3376	23.0	34	117.1	1495	8974	48.0	33	71.8	1305	6423
-1.5	222		4251	3603	23.5	34	117.2	1709	8862	48.5	32	70.5	1571	6544
-1.0	555		4718	3337	24.0	34	117.4	1965	9046	49.0	33	70.7	1860	6234
-0.5	544		3805	2940	24.5	32	117.8	1937	8437	49.5	22	68.4	1873	5871
0.0	544		1086	1511	25.0	34	113.9	2075	7748	50.0	41	70.1	1749	6114
0.5	554		2430	3303	25.5	33	116.7	2272	7848	50.5	32	69.3	1561	6126
1.0	655		3309	4333	26.0	33	115.9	2327	8298	51.0	32	68.5	1752	6115
1.5	332		3518	4723	26.5	33	114.5	2209	8220	51.5	32	68.7	1863	5880
2.0	333		3367	4498	27.0	34	111.9	2289	7988	52.0	22	67.7	1660	5788
2.5	333		3172	4246	27.5	33	109.7	2096	7558	52.5	33	67.3	1936	5453
3.0	332		3187	4444	28.0	35	110.9	1901	7769	53.0	33	64.2	2308	5191
3.5	333		3248	4455	28.5	34	110.0	1939	8178	53.5	33	62.2	2381	5040
4.0	332		3153	4297	29.0	33	108.7	1760	8534	54.0	23	59.7	2311	4788
4.5	322		2985	4279	29.5	13	109.3	1585	8823	54.5	31	54.6	2204	4293
5.0	313		3003	4533	30.0	33	113.6	1634	8938	55.0	32	50.8	1864	4316
5.5	323		2934	4559	30.5	43	115.6	1937	8675	55.5	32	50.1	1721	4416
6.0	233		2709	4392	31.0	43	117.1	1983	8857	56.0	11	50.1	1772	4215
6.5	323		2705	4564	31.5	24	114.2	1770	9084	56.5	32	48.9	2097	3993
7.0	323		2834	4674	32.0	32	111.8	1616	7873	57.0	32	46.3	2320	3972
7.5	333		2678	4882	32.5	33	109.9	1572	7344	57.5	32	45.1	2329	4092
8.0	323		2496	4998	33.0	34	108.1	1437	7640	58.0	33	44.9	2333	4139
8.5	323		2497	4948	33.5	33	107.7	1590	8190	58.5	33	44.7	2390	3890
9.0	332		2390	4937	34.0	34	107.3	1669	8135	59.0	23	44.0	2841	3651
9.5	332		2533	5275	34.5	33	106.0	1596	7779	59.5	33	43.1	3114	3533
10.0	232		2634	5885	35.0	22	102.5	1575	7364	60.0	23	41.4	3023	3401
10.5	223		2410	6467	35.5	24	98.4	1610	7310	60.5	33	40.9	3017	3253
11.0	333		2200	6352	36.0	24	94.9	1465	7171	61.0	32	39.0	3080	3080
11.5	234		2186	6459	36.5	24	93.2	1733	7292	61.5	33	37.8	3143	3240
12.0	433		2172	7075	37.0	44	93.7	1847	7727	62.0	32	35.8	2683	3323
12.5	23		2250	6937	37.5	44	93.9	1917	7995	62.5	23	45.3	2479	3438
13.0	33		2075	6477	38.0	34	93.6	2186	8256	63.0	23	45.7	2422	3367
13.5	33		1917	6594	38.5	34	92.5	2365	8301	63.5	42	34.8	2297	3145
14.0	33		2013	6835	39.0	32	90.8	2612	8206	64.0	33	31.3	2349	2952
14.5	33		1786	6851	39.5	22	89.1	2439	7973	64.5	33	29.6	2658	2848
15.0	32		1610	7206	40.0	22	83.0	2128	7721	65.0	32	28.8	2950	2867
15.5	31		1561	6819	40.5	32	81.4	2029	7208	65.5	14	26.8	2901	2745
16.0	32	146.6	1580	6684	41.0	31	78.8	2129	7032	66.0	13	26.2	2576	2762
16.5	34	144.2	1756	6722	41.5	32	77.0	1946	7104	66.5	23	22.7	2516	2550
17.0	34	139.8	2211	6793	42.0	31	76.1	2276	7177	67.0	33	21.0	2455	2414
17.5	33	138.1	2229	6814	42.5	32	77.2	2295	6983	67.5	33	21.3	2322	2384
18.0	33	135.3	2170	7085	43.0	22	78.3	2077	6766	68.0	33	20.8	2251	2460
18.5	33	132.7	2254	7833	43.5	22	76.2	1840	6662	68.5	32	20.6	2414	2588

Table 3 (continued)

l	Cov.	V_t (km s^{-1})	B_n ($^{\circ}\text{K km s}^{-1}$)	B_p	l	Cov.	V_t (km s^{-1})	B_n ($^{\circ}\text{K km s}^{-1}$)	B_p	l	Cov.	V_t (km s^{-1})	B_n ($^{\circ}\text{K km s}^{-1}$)	B_p
69.0	33	20.8	2610	2626	89.0	23	14.7	4491	757	109.0	33	3.9	3862	384
69.5	33	20.9	2871	2620	89.5	23	13.0	4608	796	109.5	32	4.2	3625	374
70.0	23	19.5	3006	2395	90.0	23	12.1	4238	879	110.0	33	4.4	3625	367
70.5	33	18.9	3242	2318	90.5	33	11.1	4030	890	110.5	33	4.9	4129	390
71.0	33	17.2	3266	2164	91.0	33	11.1	4090	921	111.0	32	5.5	4147	412
71.5	33	17.2	3160	2101	91.5	23	11.0	3997	998	111.5	33	5.7	4057	408
72.0	32	17.0	3218	2029	92.0	33	10.4	4018	947	112.0	32	6.2	3979	419
72.5	32	16.7	3140	2039	92.5	32	9.7	4039	822	112.5	32	6.1	3774	410
73.0	12	16.0	3242	1975	93.0	33	9.8	4407	764	113.0	32	6.1	3481	396
73.5	32	14.3	3323	1848	93.5	24	10.6	4620	822	113.5	33	6.5	3347	389
74.0	32	14.5	3554	1783	94.0	33	9.9	4803	785	114.0	33	7.0	3825	406
74.5	32	14.0	3632	1761	94.5	33	9.8	4997	759	114.5	22	7.2	4101	422
75.0	32	13.6	3718	1673	95.0	33	10.3	4974	701	115.0	13	7.1	3991	424
75.5	32	14.1	3653	1622	95.5	23	10.3	4949	644	115.5	23	6.1	3747	388
76.0	33	14.3	3711	1620	96.0	32	9.9	4744	598	116.0	22	5.6	3689	382
76.5	32	14.3	4102	1572	96.5	33	9.2	4460	545	116.5	22	5.7	3311	383
77.0	32	14.6	4575	1589	97.0	33	8.5	4184	540	117.0	32	6.1	3047	400
77.5	22	15.7	4726	1756	97.5	23	8.2	4249	537	117.5	32	6.2	3067	402
78.0	22	17.9	4610	1965	98.0	33	7.7	4412	518	118.0	22	6.2	3090	407
78.5	32	20.5	4584	1960	98.5	32	7.7	4563	499	118.5	22	6.3	3135	408
79.0	32	20.6	4365	2028	99.0	32	8.3	4406	518	119.0	22	6.4	3434	393
79.5	32	18.9	3932	2080	99.5	33	8.5	4130	545	119.5	22	6.3	3741	382
80.0	31	17.5	3434	1881	100.0	33	8.5	3851	562	120.0	22	6.4	4074	388
80.5	32	16.8	3290	1788	100.5	32	8.0	3646	554					
81.0	12	18.1	3500	1897	101.0	33	7.8	3435	549					
81.5	31	19.8	3693	1948	101.5	33	7.6	3455	528					
82.0	32	20.4	3740	2014	102.0	33	7.0	3565	505					
82.5	32	18.5	3763	2018	102.5	32	6.2	3663	450					
83.0	32	17.3	3769	1829	103.0	33	5.8	3811	438					
83.5	32	17.1	3584	1608	103.5	33	5.9	3769	440					
84.0	33	17.0	3872	1478	104.0	33	6.3	3800	450					
84.5	33	16.1	4280	1341	104.5	33	6.3	3521	453					
85.0	33	15.1	4225	1192	105.0	33	6.5	3433	462					
85.5	33	14.2	4094	1093	105.5	33	6.3	3503	452					
86.0	23	14.9	4473	946	106.0	33	6.1	3598	438					
86.5	22	14.6	4434	872	106.5	33	5.2	3699	410					
87.0	22	14.4	4018	865	107.0	33	4.7	3909	394					
87.5	22	15.3	3762	720	107.5	33	4.1	3962	371					
88.0	22	15.8	4003	650	108.0	32	3.6	3890	355					
88.5	22	15.3	4175	646	108.5	33	3.8	3954	358					

Table 4. Observed velocity ranges

Longitude range	V_{\min}	V_{\max}	Longitude range	V_{\min}	V_{\max}
	(km s ⁻¹)			(km s ⁻¹)	
$-6.0 \leq l \leq 1.0$	-340	+280	$35.5 \leq l \leq 65.0$	-200	+220
$-1.0 \leq l \leq 6.0$	-280	+340	$65.5 \leq l \leq 85.0$	-220	+160
$6.5 \leq l \leq 12.0$	-200	+340	$85.5 \leq l \leq 120.0$	-240	+120
$12.5 \leq l \leq 35.0$	-160	+260			

REFERENCES

- Boer, J. A. de, Hin, A. C., Schwarz, U. J., Woerden, H. van 1968, *Bull. astr. Inst. Netherl.*, **19**, 460.
- Hartsuijker, A. P., Baars, J. W. M., Drenth, S., Volders, L. 1970, *Astr. Astrophys. Suppl.*, in preparation.
- Hoekema, T. 1969, *Automatische Reductie van 21-cm Lijnwaarnemingen*, Leiden Observatory.
- MacRae, D. A., Westerhout, G. 1956, *Tables for Reduction of Velocities to the Local Standard of Rest*, Lund Observatory.
- Muller, C. A., Raimond, E., Schwarz, U. J., Tolbert, C. R. 1966, *Bull. astr. Inst. Netherl. Suppl.*, **1**, 213.
- Raimond, E. 1966, *Bull. astr. Inst. Netherl. Suppl.*, **1**, 33.
- Shane, W. W., Bieger-Smith, G. P. 1966, *Bull. astr. Inst. Netherl.*, **18**, 263.
- Volders, L., Högbom, J. A. 1961, *Bull. astr. Inst. Netherl.*, **15**, 307.
- Westerhout, G. 1958, *Bull. astr. Inst. Netherl.*, **14**, 215.
- Woerden, H. van 1962, *De Neutrale Waterstof in Orion*, dissertation, Groningen Univ.
- Woerden, H. van, Takakubo, K., Braes, L. L. E. 1962, *Bull. astr. Inst. Netherl.*, **16**, 321.

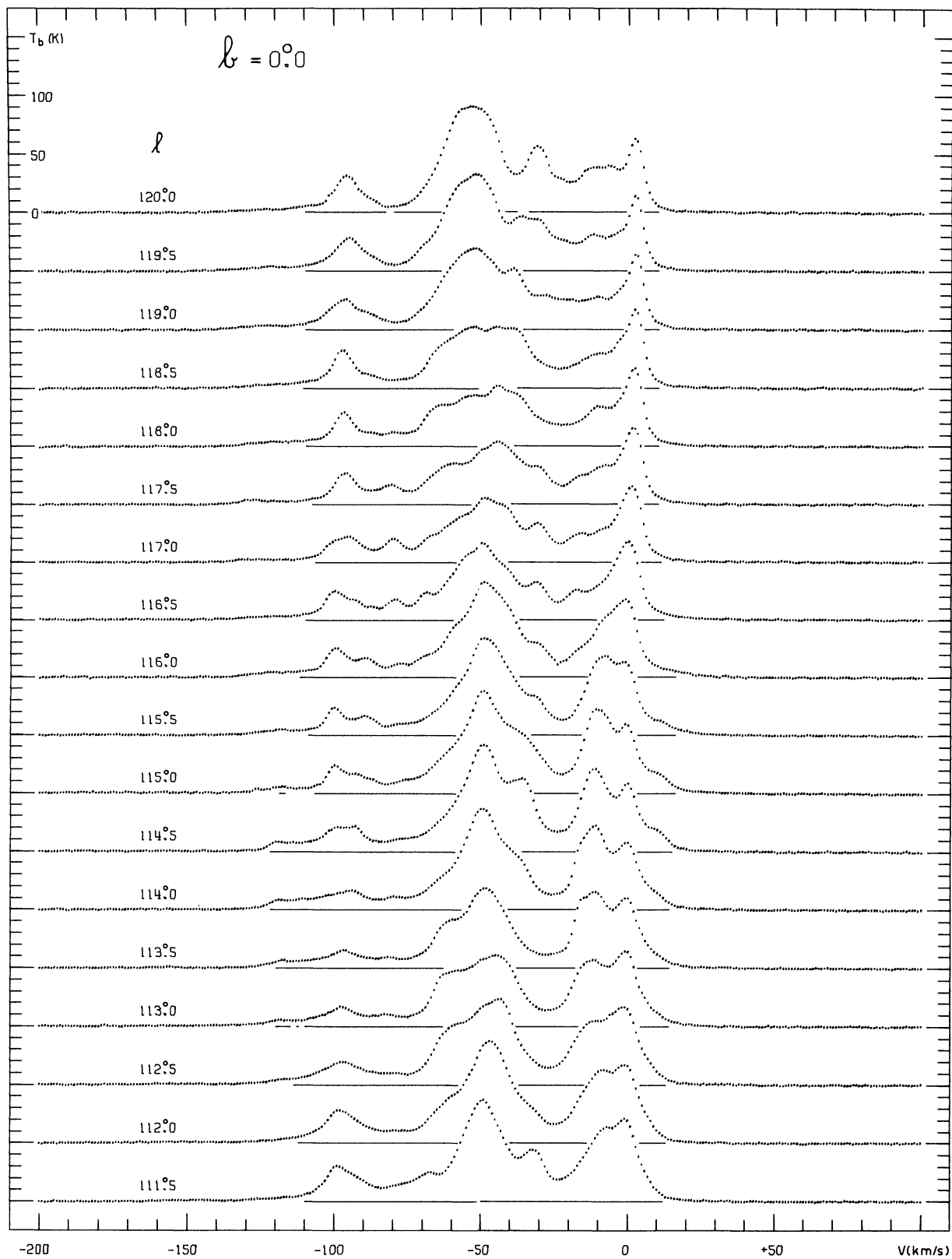
W. B. Burton

Sterrewacht, Leiden 2401, The Netherlands

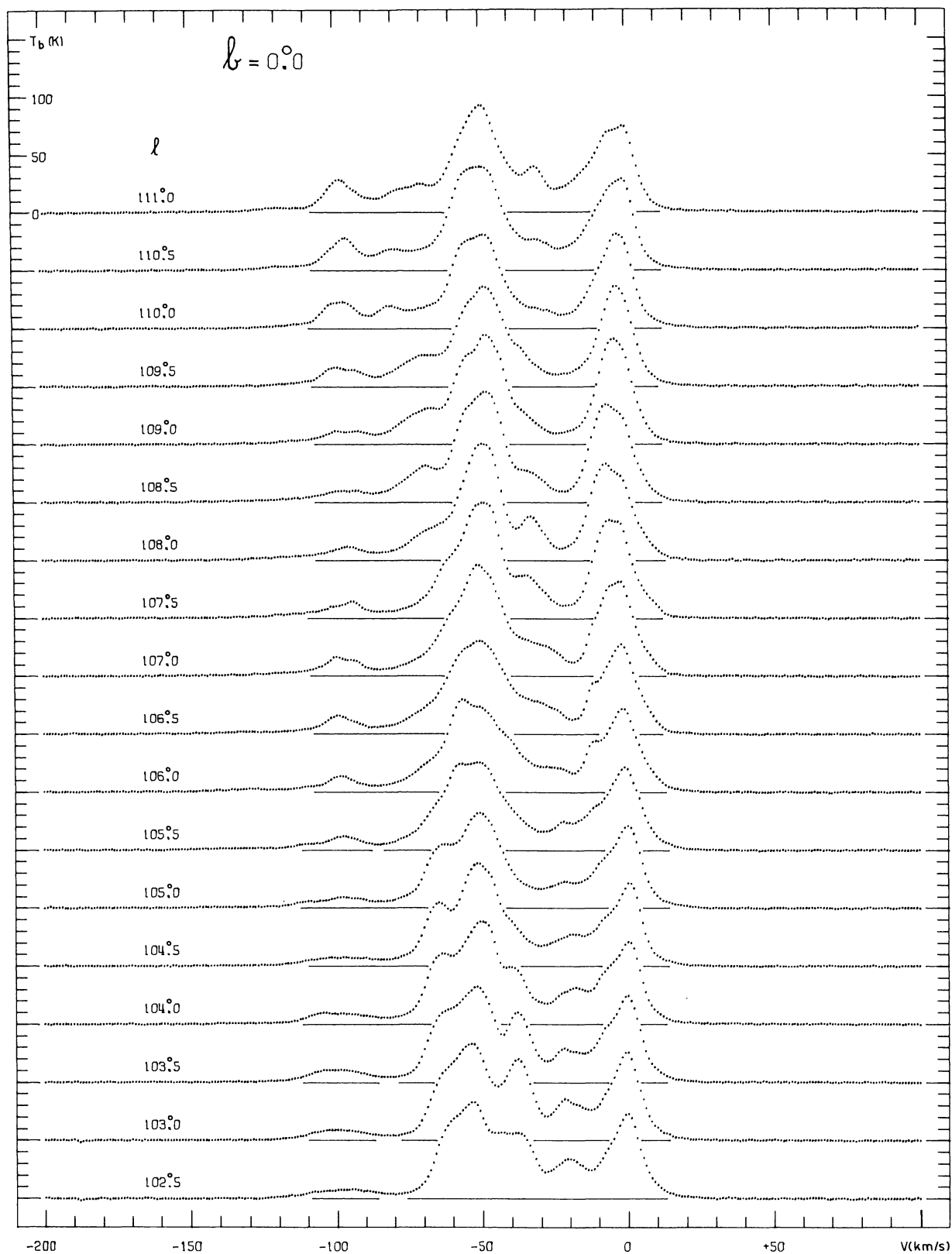
(This Page Intentionally Left Blank)

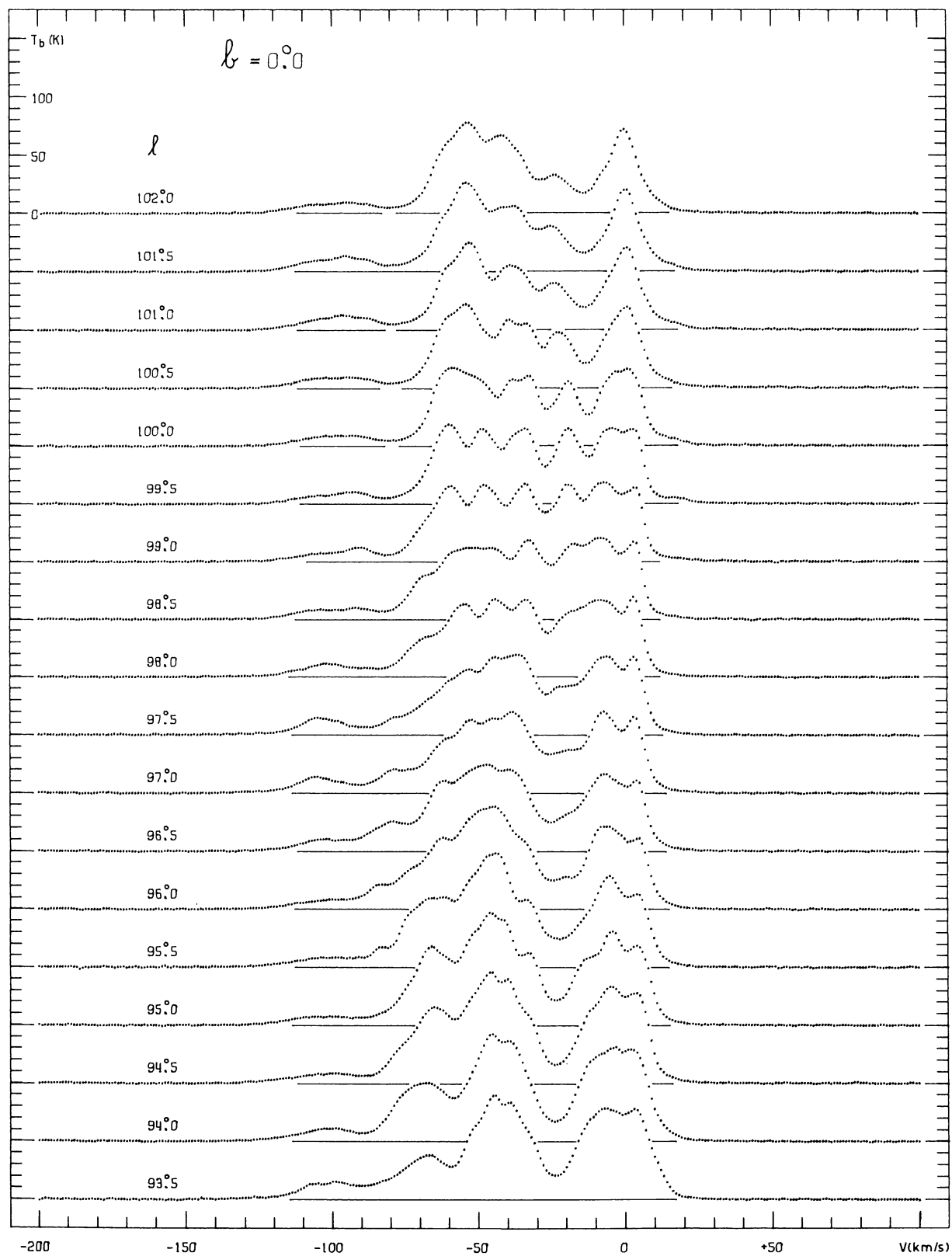
DWINGELOO ATLAS OF 21-CM PROFILES

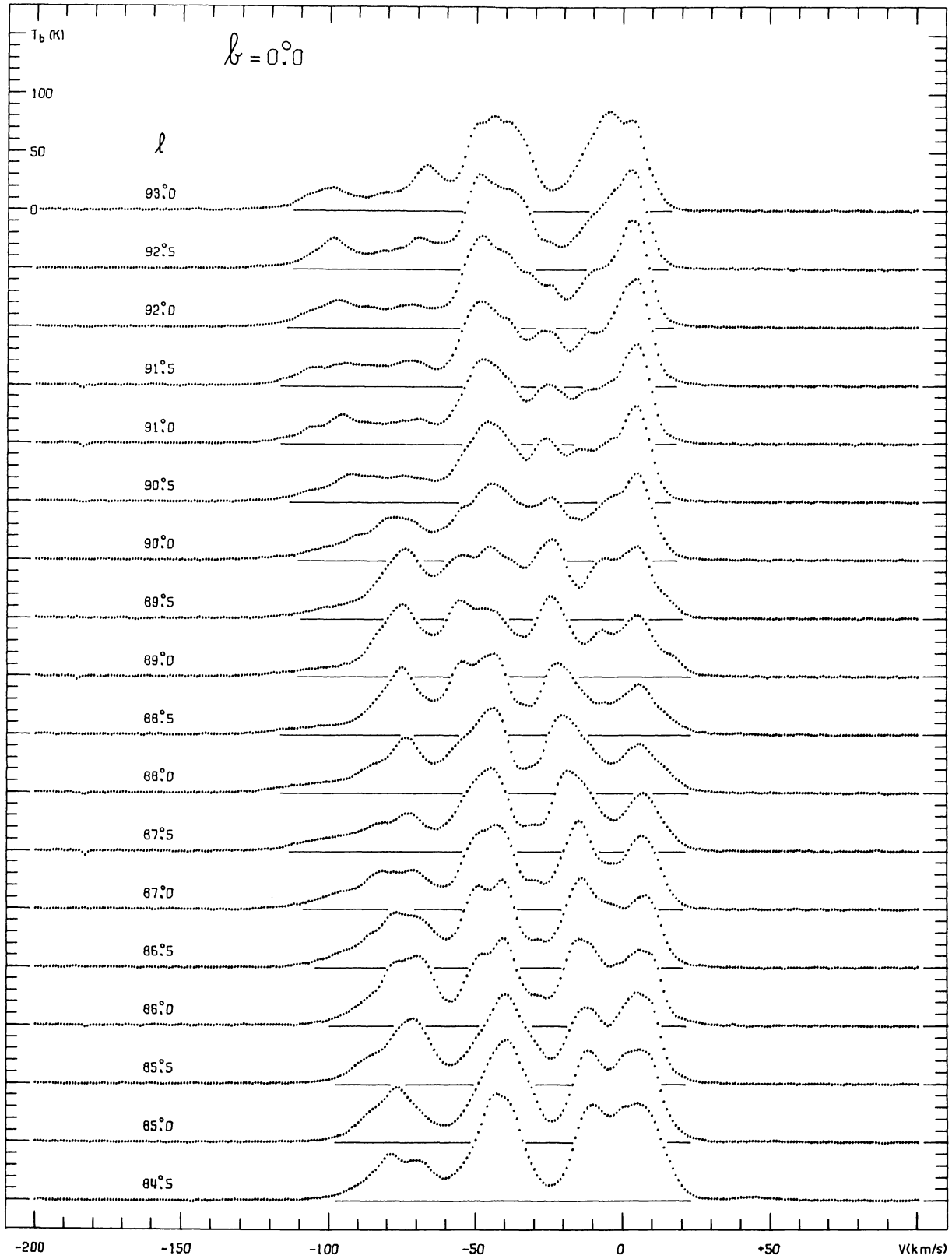
PART V

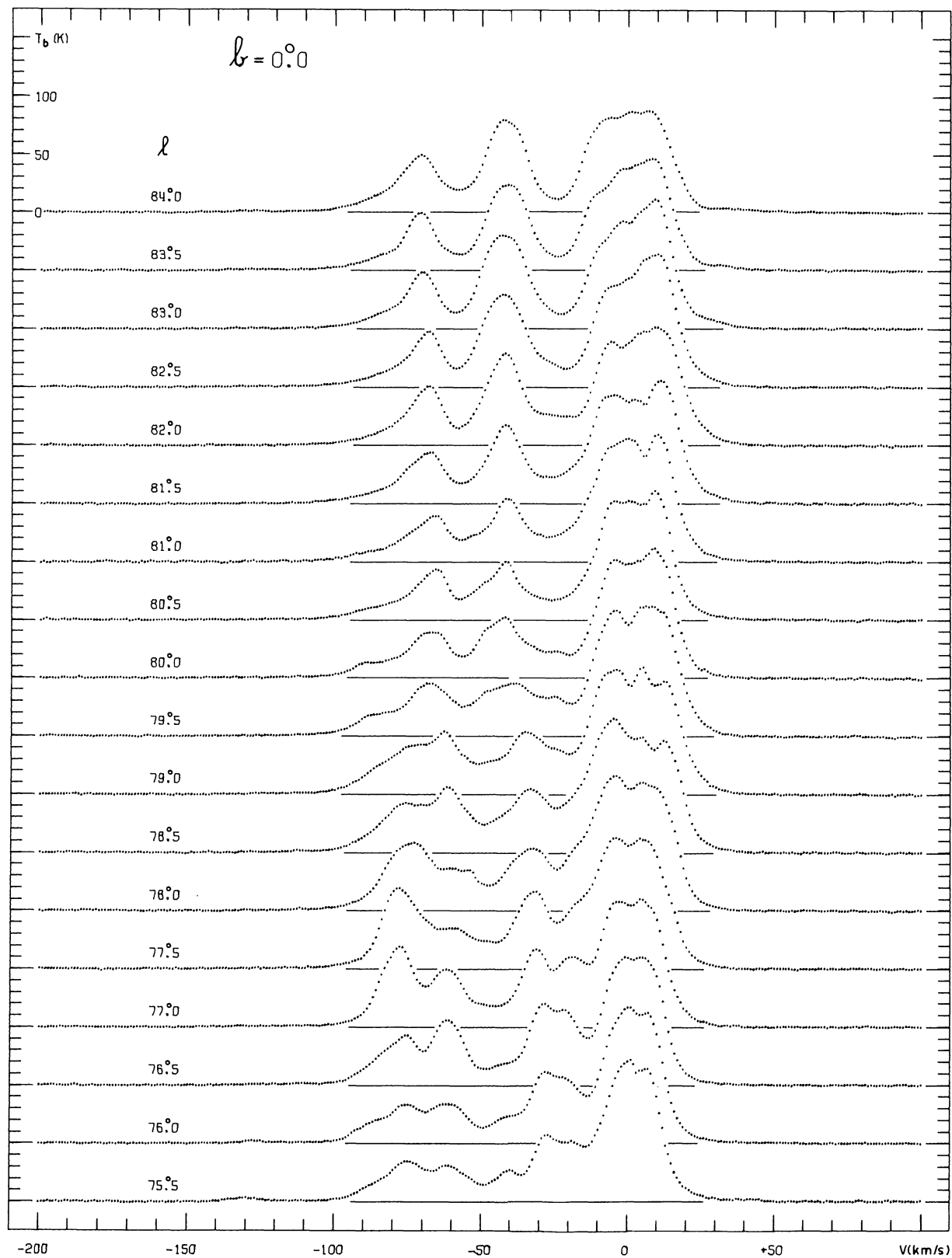


1970A&AS.....2...261B

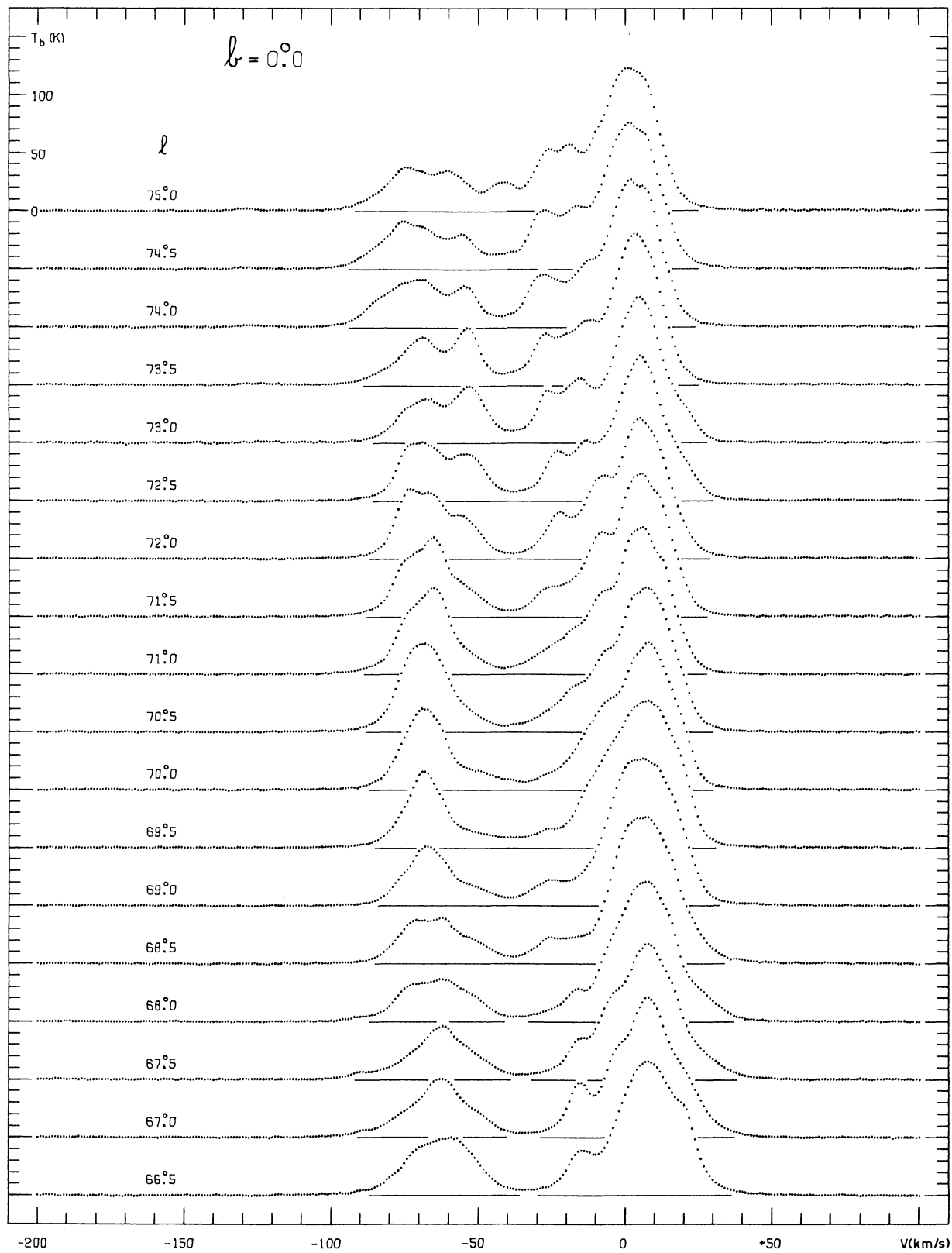


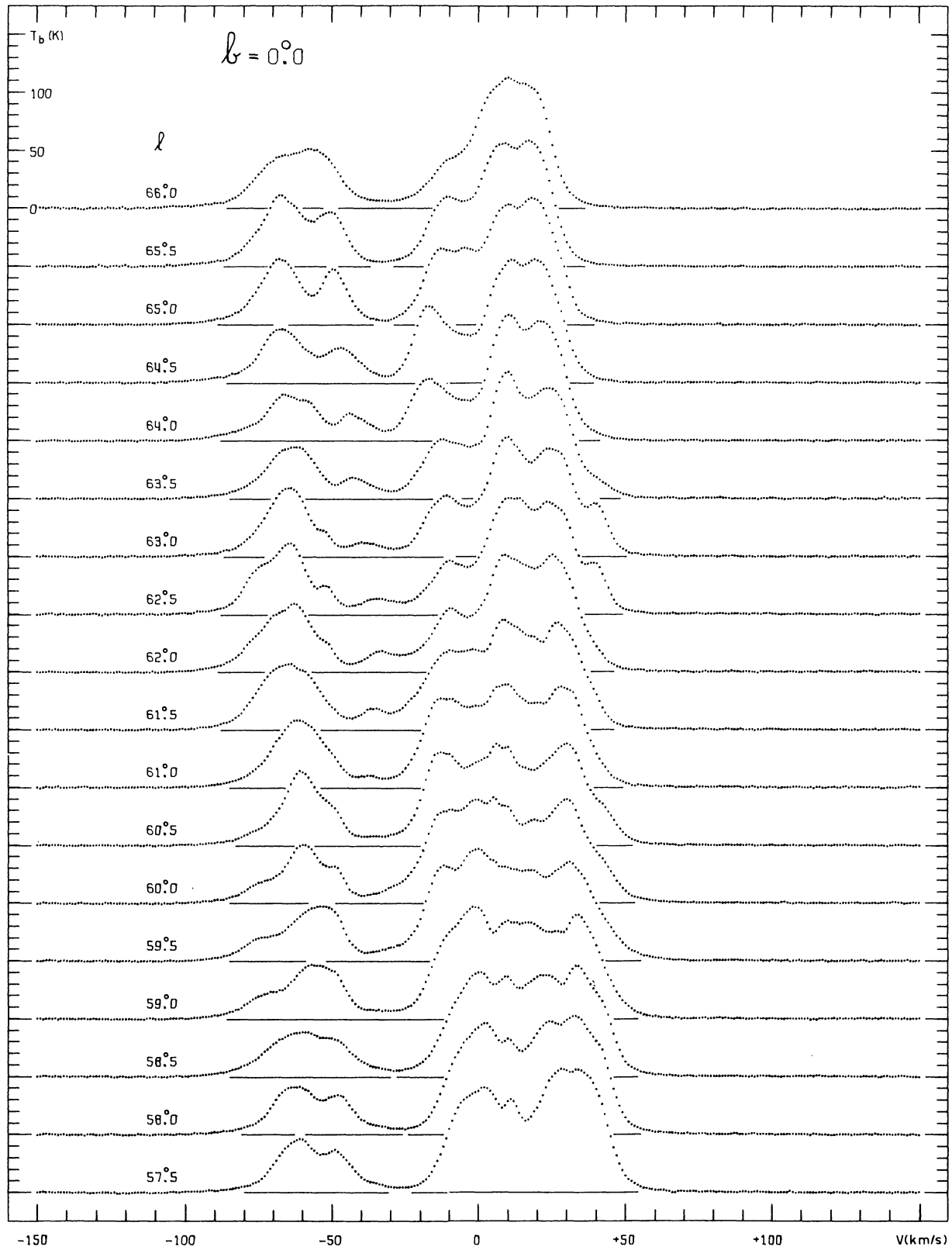




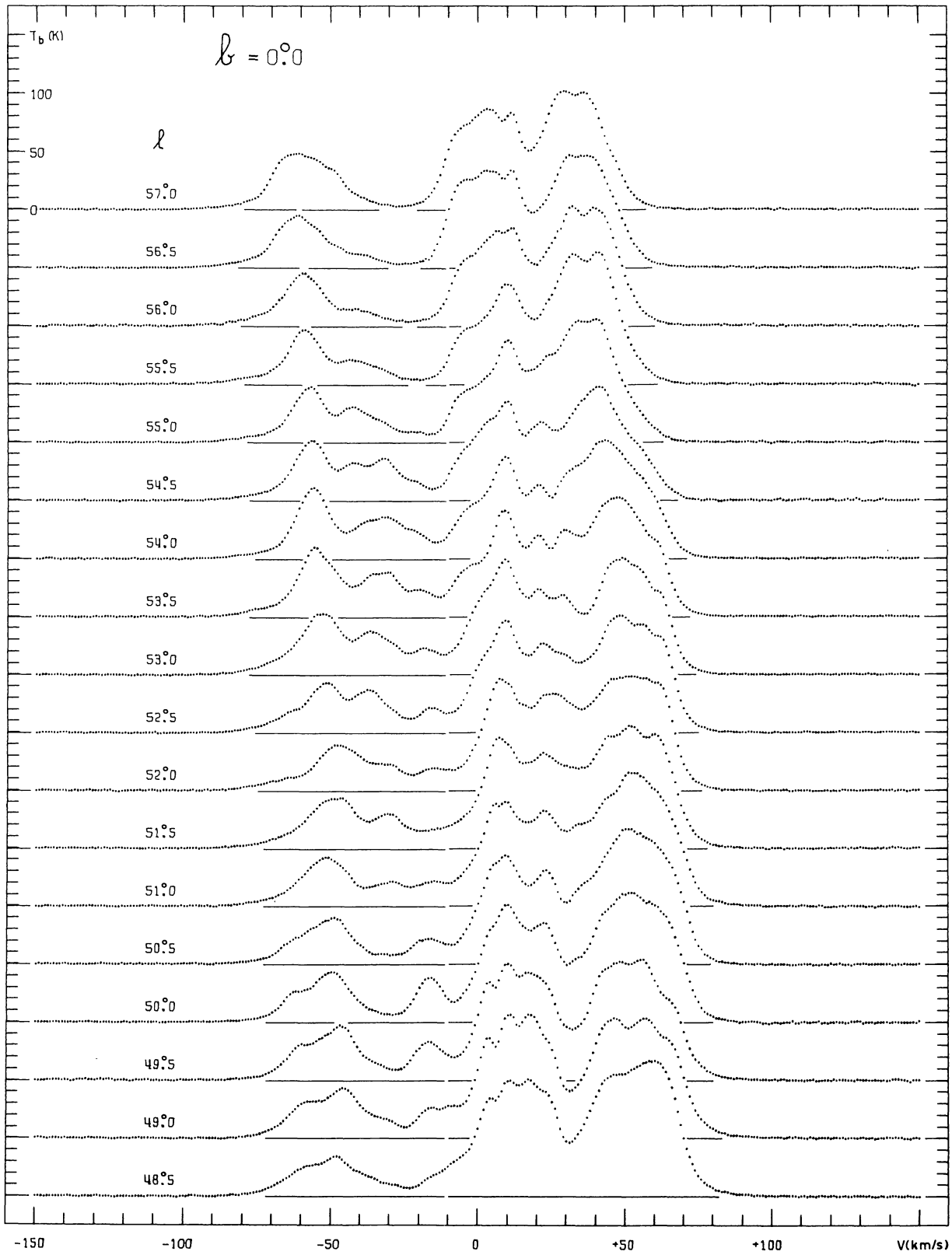


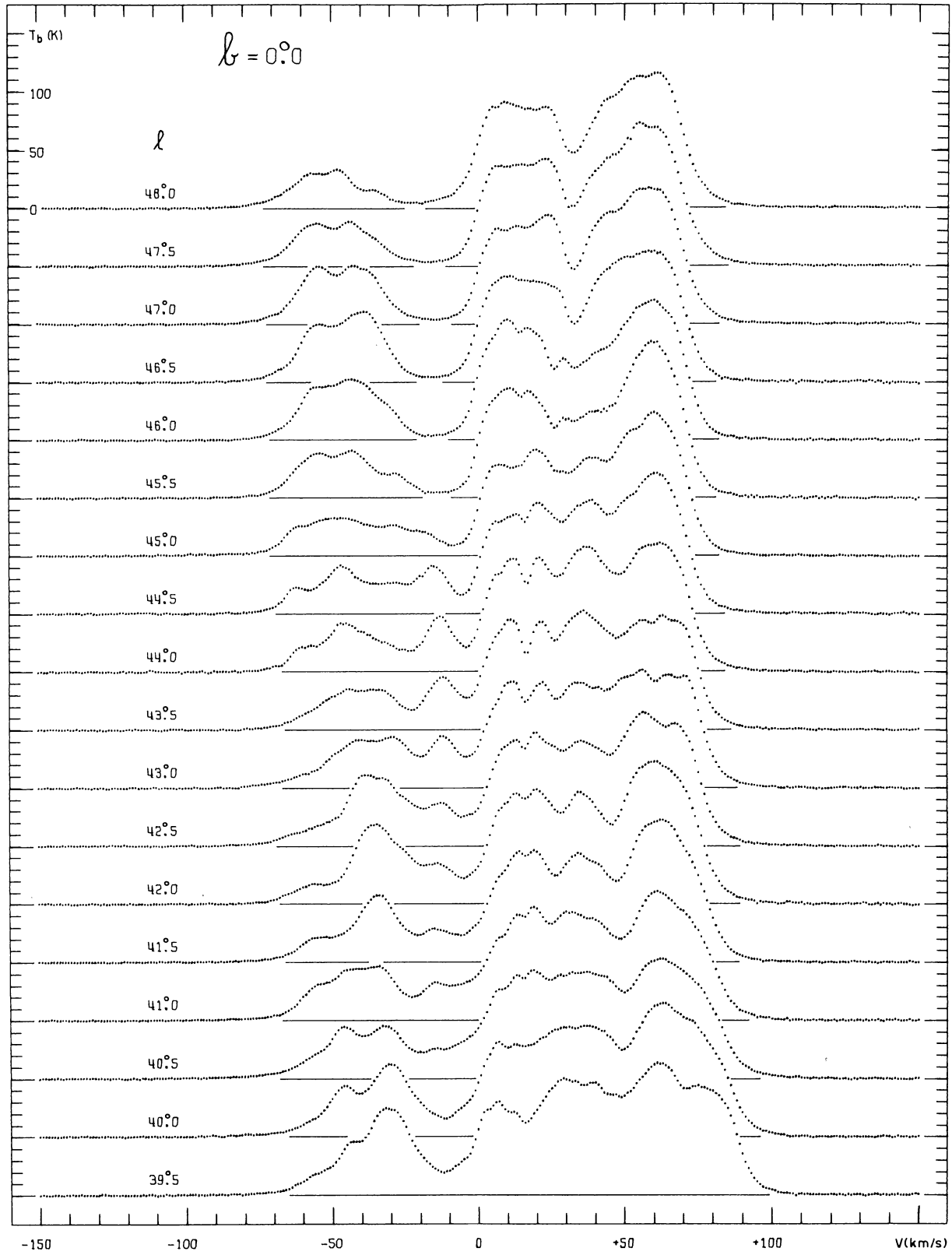
1970AEAS.....2...261B



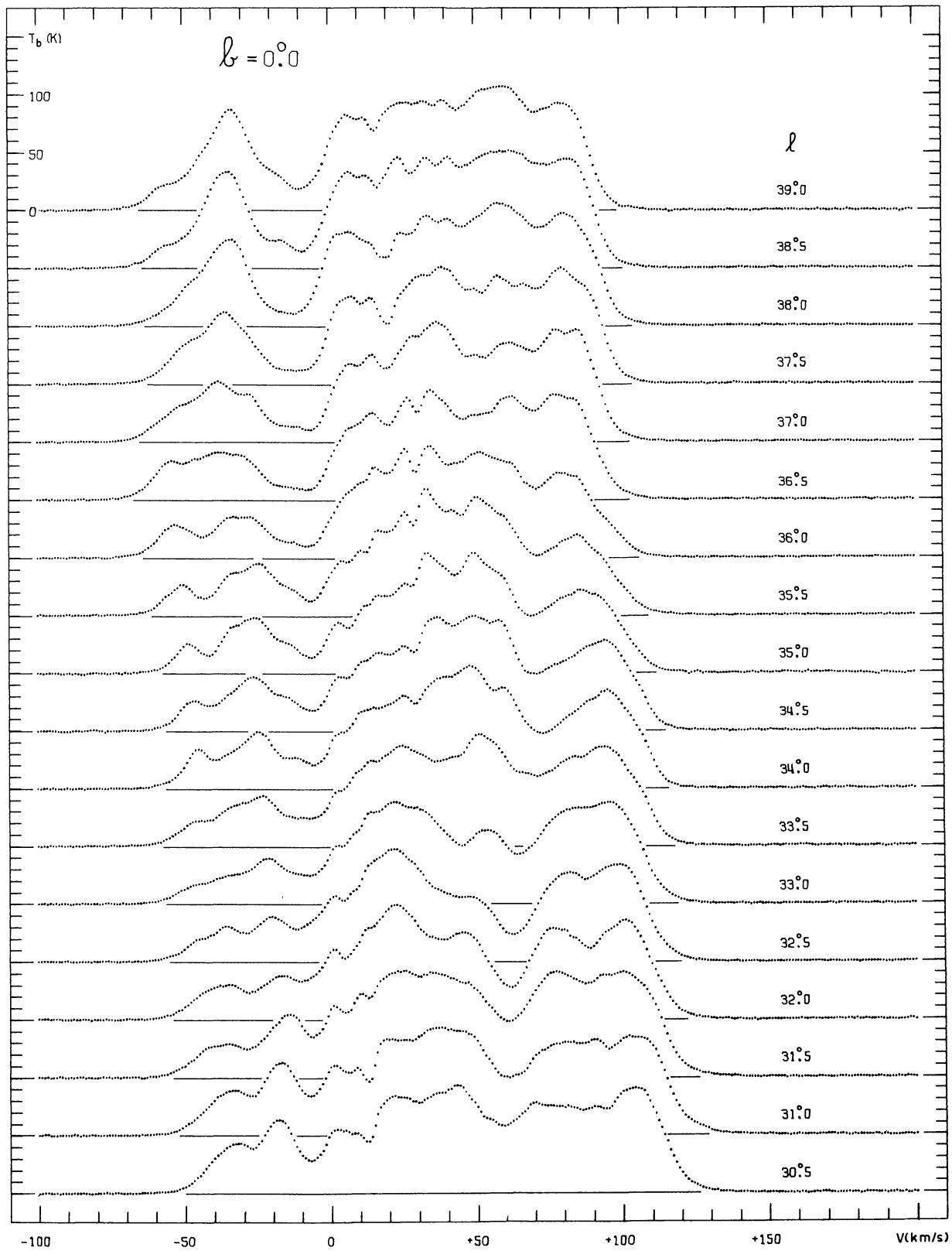


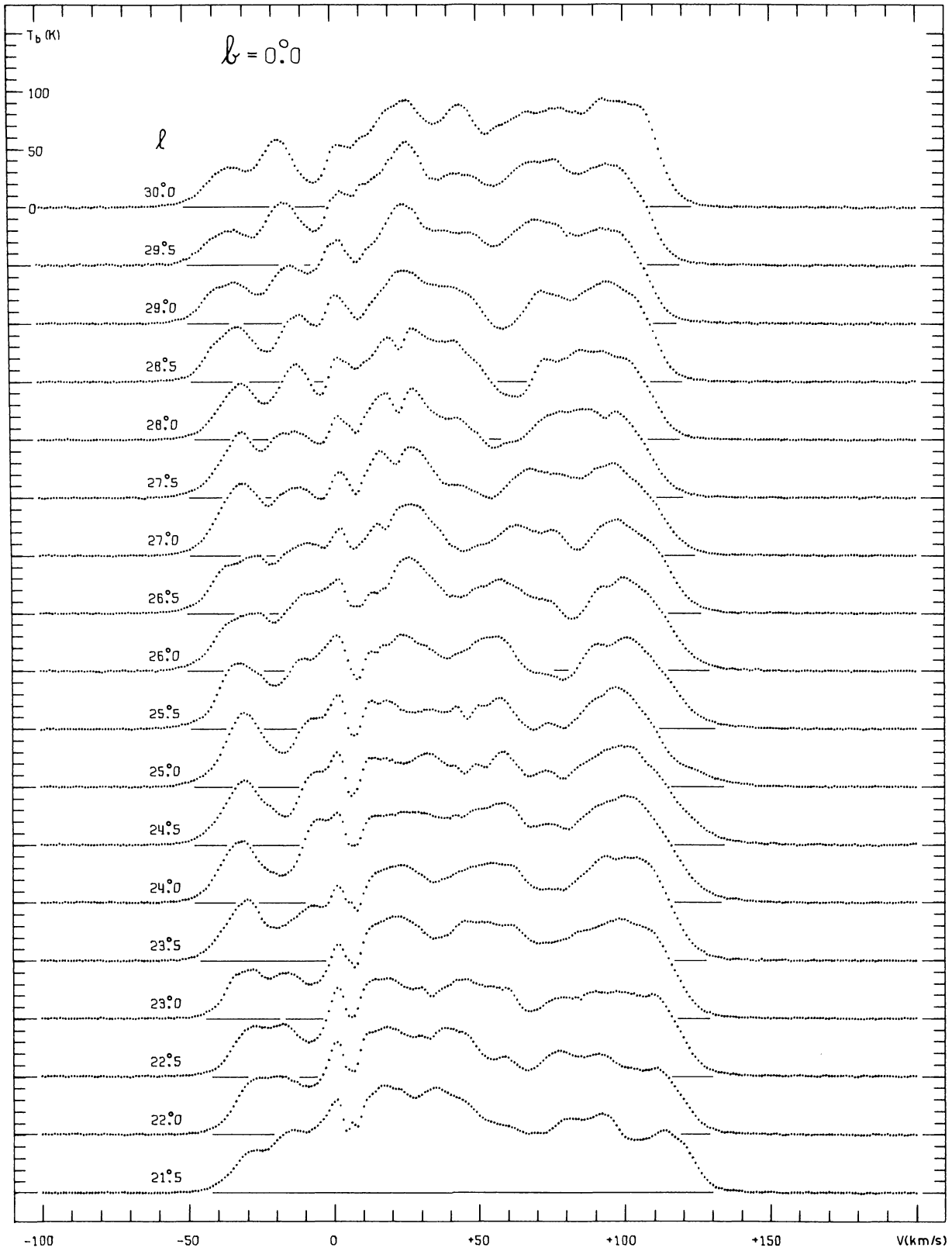
1970A&AS.....2...261B



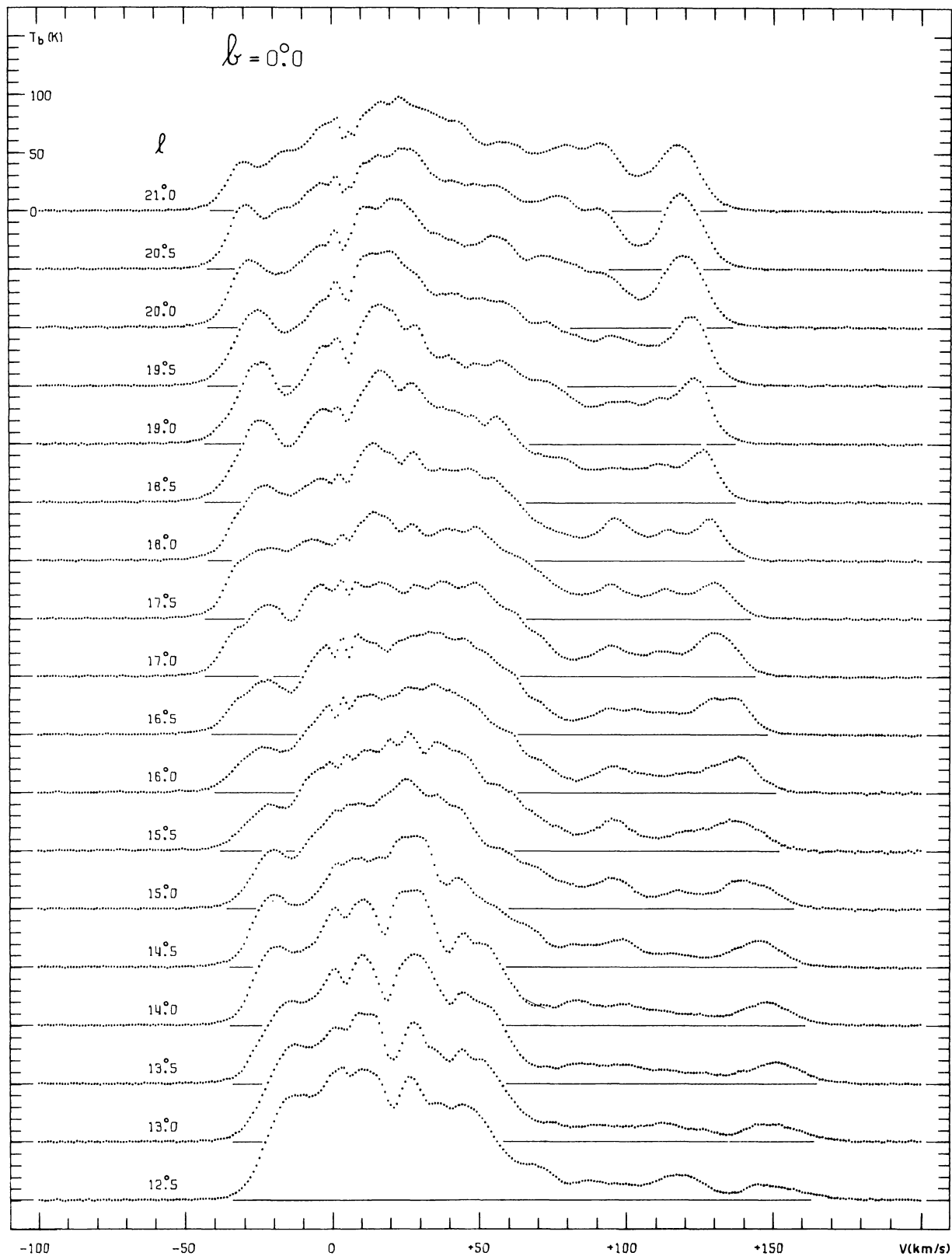


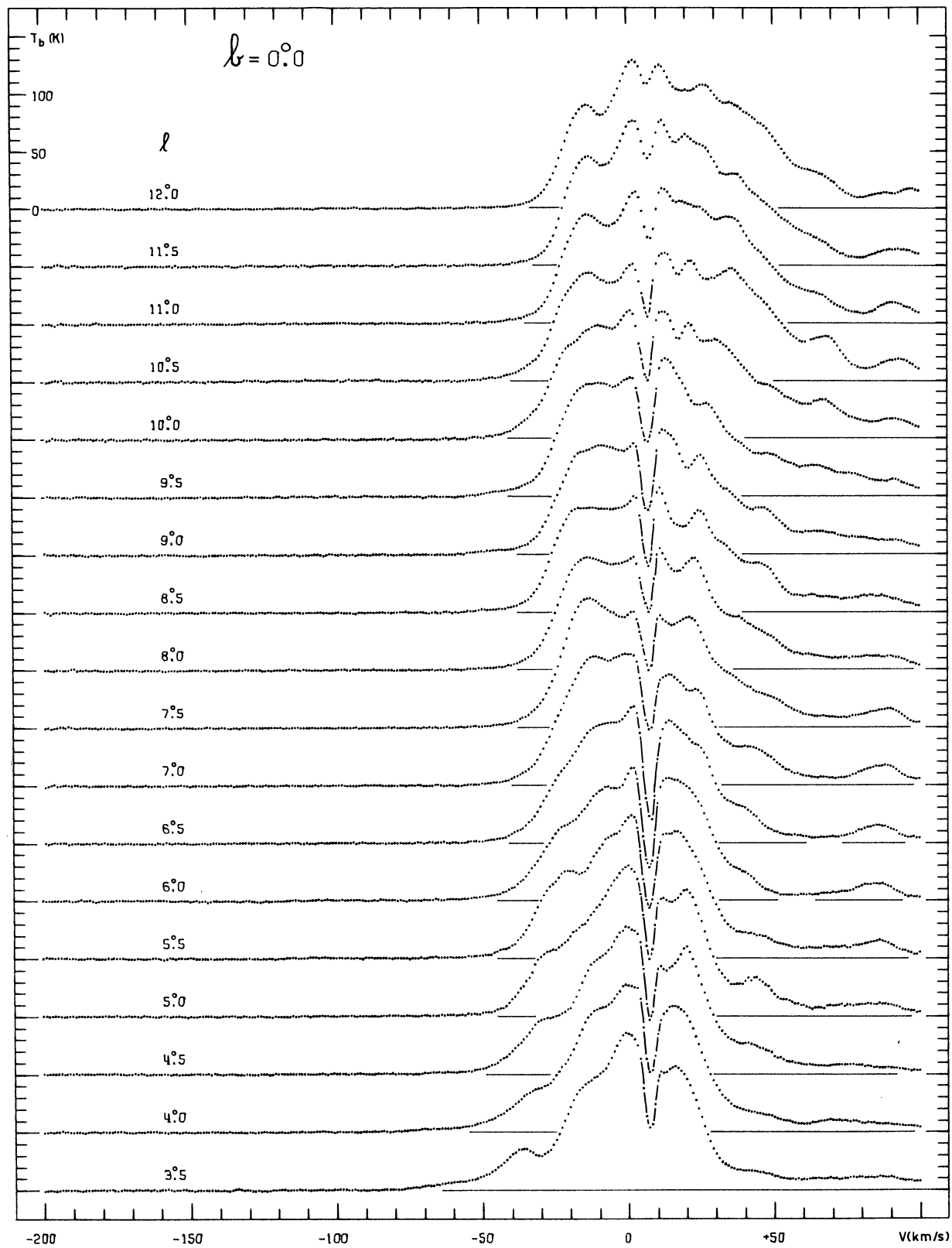
1970AEAS.....2...261B



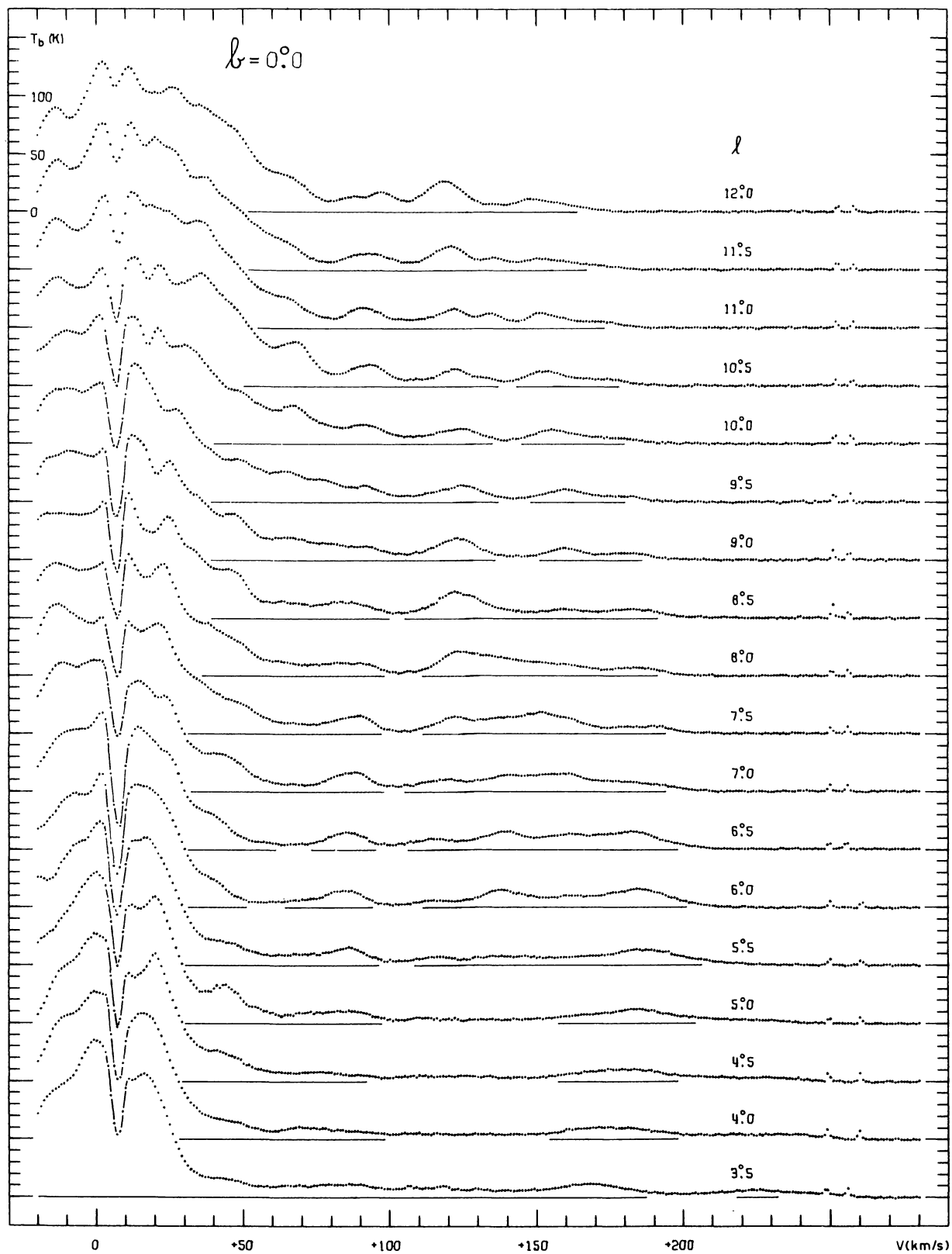


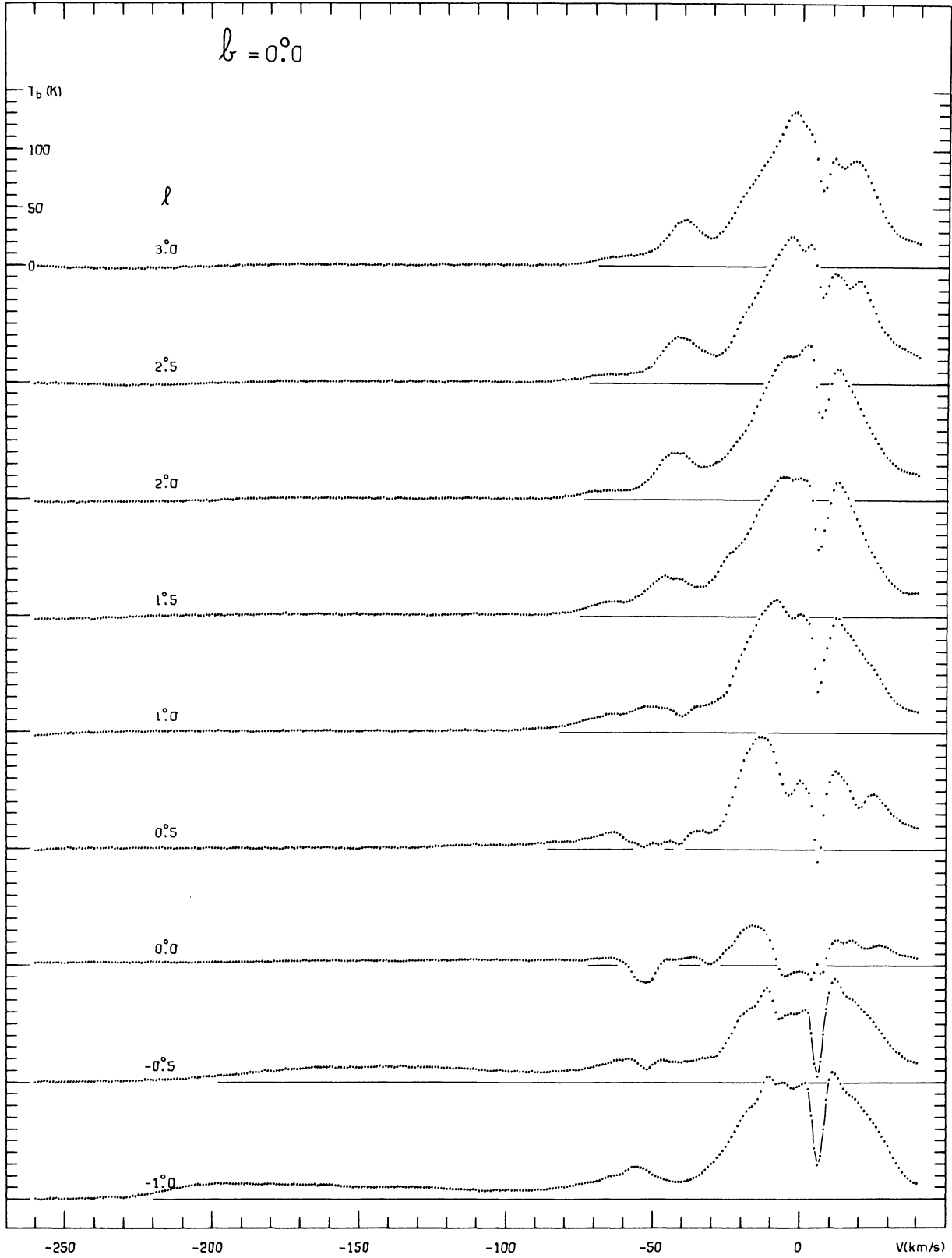
1970AEAS.....2...261B

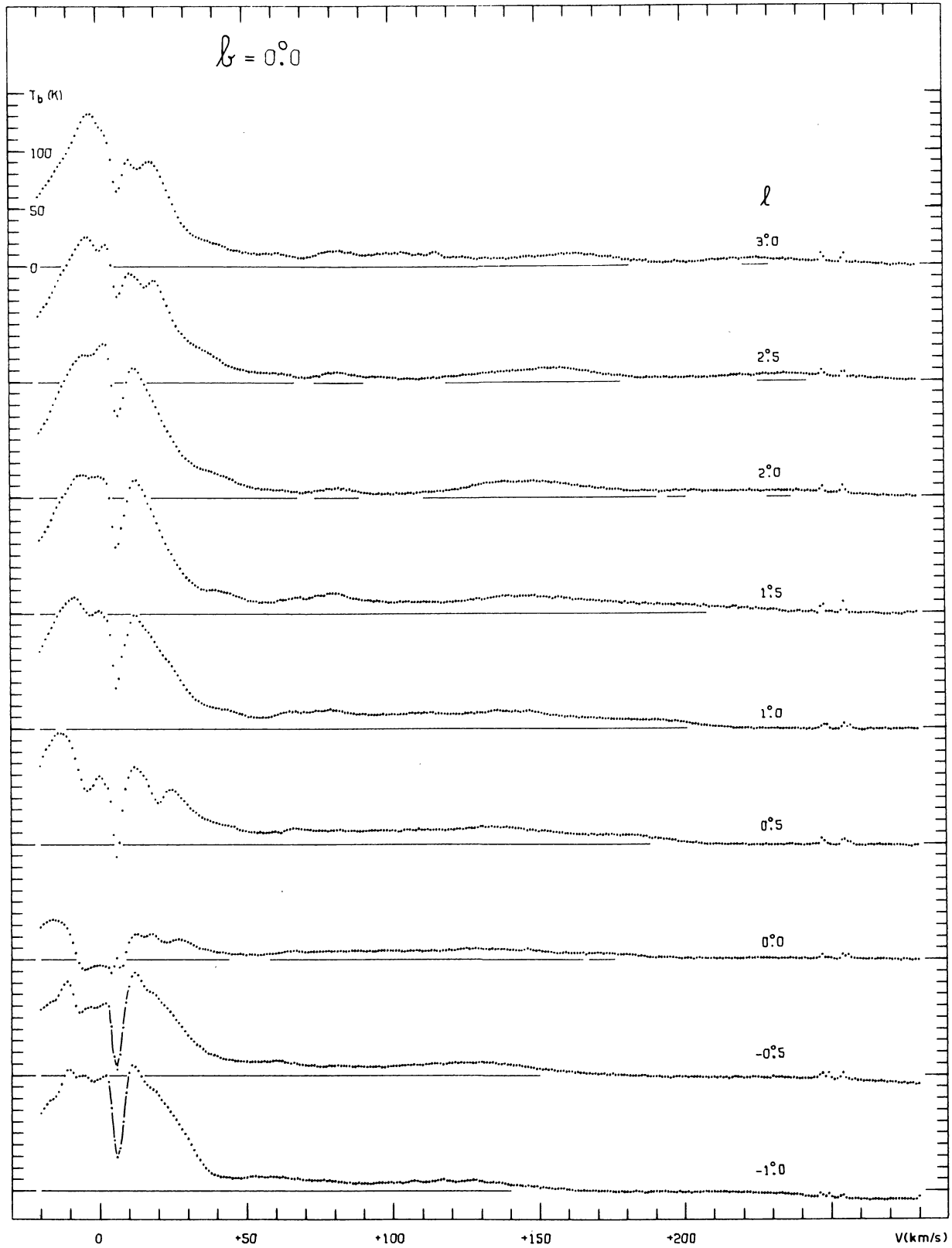


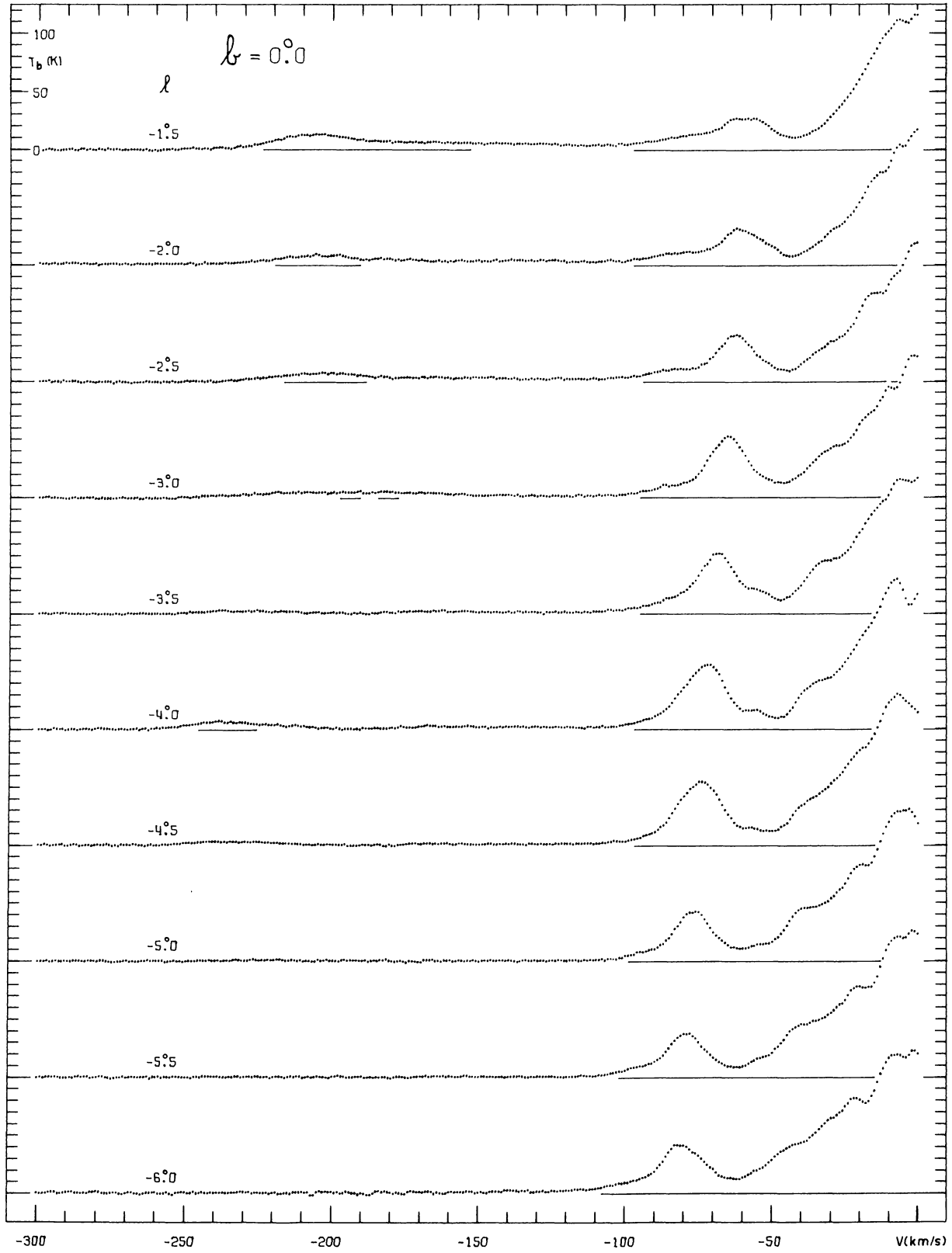


1970A&AS.....2...261B









1970AEAS.....2...261B

